Plant Physiol. (1995) 107: 1159–1166

Biogenesis and Ultrastructure of Carboxysomes from Wild Type and Mutants of *Synechococcus* sp. Strain PCC 7942[1]

María Isabel Orús*, María Luisa Rodríguez, Flor Martínez, and Eduardo Marco

Departamento de Biología, Facultad de Ciencias, Universidad Autónoma de Madrid, 28049 Madrid, Spain

Immature inclusions representing three progressive steps of carboxysome biogenesis have been identified in *Synechococcus* during the period of adaptation to low-CO_2 conditions: (a) ring-shaped structures, (b) electron-translucent inclusions with the shape of a carboxysome and the internal orderly arrangement of ribulose-1,5-bisphosphate carboxylase oxygenase (Rubisco) molecules, and (c) carboxysomes with an internal electron-translucent area, which seem to be the penultimate stage of carboxysome maturation. The ability to build up normal carboxysomes is impaired in three (M3, EK6, and D4) of four high-carbon-requiring mutants studied in this work. M3 and EK6 exhibit abundant immature electron-translucent carboxysomes but no mature ones. This finding supports the contention that an open reading frame located 7.5 kb upstream of the gene encoding the large subunit of Rubisco (altered in M3) is involved in the carboxysome composition and confirms the structural role of the small subunit of Rubisco (slightly modified in EK6) in the assembly of these structures. D4 shows few typical carboxysomes and frequent immature types, its genetic lesion affecting the apparently unrelated gene encoding a subunit of phosphoribosyl aminoamidazole carboxylase of the purine biosynthesis pathway. Revertants EK20 (EK6) and RK13 (D4) have normal carboxysomes, which means that the restoration of the ability to grow under low CO_2 coincides with the proper assembling of these structures. N5, a transport mutant due to the alteration of the gene encoding subunit 2 of NADH dehydrogenase, shows an increase in the number and size of carboxysomes and frequent bar-shaped ones.

Carboxysomes are currently under intense investigation due to the central role assigned to these polyhedral bodies in the adaptation of cyanobacteria to changes in ambient CO_2 concentration via the induction of the CCM (Reinhold et al., 1989, 1991). The CCM enables cyanobacteria to fix CO_2 efficiently even when the external dissolved CO_2 concentration is in equilibrium with air, a condition that should theoretically be limiting because of the low affinity of cyanobacterial Rubisco for this substrate (Badger, 1980).

Intracellular concentrations of C_i up to 1000-fold higher than the external C_i, a rise of 10- to 20-fold in the apparent photosynthetic affinity for external C_i, and an increase in the number of carboxysomes are relevant features involved in the operation of this mechanism (Badger and Price, 1992). Mutants that require elevated levels of CO_2 for growth, the so-called HCRMs, are being used to investigate the various components of the process of adaptation. A number of HCRMs of *Synechococcus* PCC 7942 have been characterized whose genomic lesions involve ORFs located in the DNA region surrounding the Rubisco operon (*rbcLS*), and some of these mutants are defective in the expression of carboxysomes (for a recent review, see Kaplan et al., 1994). However, there are also HCRMs whose DNA lesions are located elsewhere, such as Tm17 (Yu et al., 1994) and G7 (Ogawa et al., 1994). G7 is a mutant of *Synechocystis* PCC 6803 that lacks carboxysomes or related structures.

Carboxysomes are supposed to play a main role in the CCM as the site where the HCO_3^- accumulated in the cytoplasm is dehydrated in situ to CO_2 by means of a carboxysomal carbonic anhydrase and supplied directly to the carboxysomal Rubisco (Reinhold et al., 1989, 1991). A great deal of evidence supporting this model has accumulated during the last years, including the identification of the *icfA* gene that encodes carboxysomal carbonic anhydrase (Fukuzawa et al., 1992; Yu et al., 1992), whose alteration results in the HCRM phenotype (Price et al., 1992) and the immunolocalization of most of cellular Rubisco in these polyhedral bodies (McKay et al., 1993). However, there is no direct confirmation of the proposed role of carboxysomes.

In recent years research has focused primarily on the physiological significance of these inclusion bodies but, to our knowledge, there are no previous reports on carboxysome biogenesis in *Synechococcus*, the cyanobacterium most frequently used in these studies.

MATERIALS AND METHODS

Organism and Growth Conditions

The wild type of *Synechococcus* PCC 7942, its HCRMs N5, M3, EK6, and D4, and the revertants EK20 and RK13 were used in this study. All of them were provided by Prof. Aaron Kaplan, who obtained the mutants by inserting a gene conferring Km^r (*nptII*) into selected sites of the genomic region of *rbcLS*, the operon encoding the large and small subunits of Rubisco (see Table I).

Batch cultures were grown in BG-11 liquid medium (Rippka, 1988) buffered with 20 mM Hepes-NaOH (pH 7.8)

[1] This work was supported by a grant from the Dirección General de Investigación Científica y Técnica of Spain (DGICYT PB90–205).

* Corresponding author; e-mail flor@vm1.sdi.vam.es; fax 34–1–3978344.

Abbreviations: CCM, carbon-concentrating mechanism; C_i, inorganic carbon; HCRM, high-carbon-requiring mutants; Km^r, kanamycin resistance; ORF, open reading frame.

Table I. *Mutant and revertants of Synechococcus PCC 7942 used in this work*

Mutant/Revertant	Genetic Lesion	Reference
HCRM N5	Km^r insert at the *Eco*RI site 12.4 kb upstream of the *rbcLS* operon (*ndhB*)	Marco et al., 1993
HCRM M3	Km^r insert at the *Eco*RI site 7.5 kb upstream of the *rbcLS* operon	Schwarz et al., 1992b
HCRM EK6	Km^r insert at *rbcS* 5 bp upstream of the stop codon	Lieman-Hurwitz et al., 1991
HCRM D4	Substitution of the 1.4-kb *PstI* of *purK*, located immediately downstream of *rbcLS*, by Km^r cartridge	Schwarz et al., 1992a
Revertant EK20	Kanamycin-resistant revertant of EK6	Lieman-Hurwitz et al., 1991
Revertant RK13	Kanamycin-resistant revertant of HCRM RK12, which had the same deletion and phenotype as D4	Lieman-Hurwitz et al., 1991

under 110 $\mu E\ m^{-2}\ s^{-1}$ continuous illumination, at 28°C, and bubbled with 5% (v/v) CO_2-enriched air (high CO_2). When indicated, culture aeration was changed to air bubbling (low CO_2) for 6, 12, or 24 h before collection.

EM

For transmission EM, cells were grown on agar plates placed in a transparent plastic box provided with a continuous flow of 5% CO_2-enriched air under the same conditions described above. Twelve hours before collecting the cells, the plates were transferred to low-CO_2 conditions by changing the CO_2-enriched air to air. Preparation of cells for EM was as described by Orús and Marco (1993) and sections were observed in a Jeol JEM1010.

Samples of isolated carboxysomes (Price et al., 1992) were negatively stained by floating electroposited carbon film onto a sample drop for 3 min, followed by refloating onto 2% (w/v) aqueous solution of uranyl acetate. Scanning EM on back-scattered electron mode was made in a Zeiss DSM940A with a solid-state detector at a working distance of 7 mm.

Analytical Methods

Culture density was determined at 600 nm. For dry weight determinations, cells were collected, washed, and dried at 70°C for 24 h. For Chl determination, samples were extracted in methanol at 4°C for 24 h in darkness. The Chl content of the extract was estimated according to the spectrophotometric method of Marker (1972). Phycobiliproteins were determined at 620 nm in the supernatant of a suspension of cells treated with toluene, according to Blumwald and Tel-Or (1982). Protein concentration was determined according to Bradford (1976) and carbohydrate content was determined by the method of Dubois et al. (1956). A Hitachi (Tokyo, Japan) U-2000 spectrophotometer was used for all analytical determinations.

RESULTS

Biogenesis of Carboxysomes

Different stages of carboxysome formation can be observed in *Synechococcus* PCC 7942 (Fig. 1). The immature carboxysome types have been found in the wild-type cells grown under high CO_2 and maintained for 12 h under low-CO_2 atmosphere (air) and are abundant in some of the mutants and mutant revertants studied. These immature inclusions had already been noticed by the authors in a preliminary study with cells grown under high CO_2 exclusively.

In addition to typical carboxysomes (Fig. 1D), carboxysome-resembling electron-clear inclusions can be noticed in wild-type cells collected during adaptation to low-CO_2 conditions. These inclusions appear to have an internal organization resulting from the regular aggregation of small particles (Fig. 1B). This substructure recalls the micrographs of negatively stained and frozen hydrated carboxysomes, showing the orderly arrangement of the Rubisco molecules inside the carboxysomes (Holthuijzen et al., 1986). Although in the wild type these immature forms represent a minor percentage of total carboxysomes, they are the majority and in some cases the only kind of polyhedral bodies in some of the mutants studied in this work.

Carboxysomes with an internal electron-translucent area (Fig. 1C) and ring-shaped structures showing a clear center and an electron-denser frame (Fig. 1A) appear occasionally, both in the wild type and the mutants.

An estimation of the frequency of these four stages in the wild type and the four mutants used in this work is given in Table II. The strains that are able to produce mature carboxysomes (WT, N5, and D4) also show ring-shaped structures, electron-translucent inclusions, and carboxysomes with a small electron-clear area. The absence of mature carboxysomes in two of the mutants (M3 and EK6) coincides with 100% electron-translucent inclusions. Ring-shaped structures were not detected in M3 and EK6, although we cannot deny that they have such structures.

According to our hypothesis, the inclusions described above represent intermediate stages of carboxysome matu-

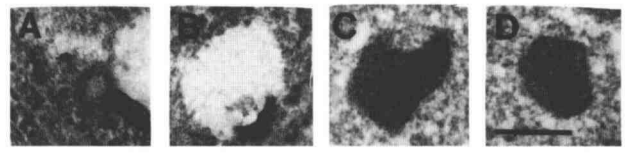

Figure 1. Transmission electron micrographs of different stages of carboxysome formation found in *Synechococcus* PCC 7942. A, Ring-shaped structure. B, Carboxysome-resembling electron-clear inclusion. C, Carboxysome with internal electron-translucent area. D, Typical mature carboxysome. Bar = 100 nm. Cells were grown under high CO_2 and changed to low-CO_2 conditions 12 h before collection.

Table II. *Carboxysome expression in wild type and HCRMs of Synechococcus PCC7942*

Cells were grown under high-CO_2 conditions and changed to low CO_2 12 h before collection.

Organism	Percentage of Cells (Sections) With/Without Carboxysomes or Related Structures		Percentage of Different Stages of Carboxysome Formation				
	With	Without	Ring-shaped structures	Carboxysome-resembling electron-clear inclusions	Carboxysomes with internal electron-clear area	Typical carboxysomes	Bar-shaped carboxysomes
Wild Type	64	36	5	19	6	70	
HCRM N5	80	20	3	9	11	63	14
HCRM M3	53	47		100			
HCRM EK6	40	60		100			
HCRM D4	48	52	2	54	7	32	5

rity; the ring-shaped structures (Fig. 1A) represent a very early stage during the biogenesis; the electron-translucent inclusions (Fig. 1B) represent a phase before that of carboxysomes with small electron-clear areas (Fig. 1C); and carboxysomes with small electron-clear areas represent the last stage leading to the mature carboxysome (Fig. 1D).

There is one observation that supports the view that the electron-translucent inclusions (Fig. 1B) are immature carboxysomes containing their main component, Rubisco molecules. Unfixed isolated carboxysome samples prepared for negative staining frequently collapse and the image obtained is of a field of Rubisco molecules. These can be identified by their "doughnut" or "double doughnut" shape in upper and side views, respectively (Fig. 2A). Highly concentrated samples of such denatured carboxysomes show that Rubisco molecules tend to self assemble (Fig. 2B), giving rise to structures clearly distinguishable from mature carboxysomes (Fig. 2C) and similar to the above-described electron-translucent inclusions (Fig. 1B).

In connection with these inclusions, a study has been made of scanning electron micrographs in back-scattered electron mode to test the possibility that such electron-clear areas are merely holes. We have compared two HCRMs, one possessing a large number of mature carboxysomes (N5) and the other lacking mature carboxysomes and showing exclusively electron-clear areas (M3). This technique (data not shown) confirms that the electron-clear areas of M3 are inclusions of less dense material that appear profusely in this mutant instead of the inclusions of dense material detected in the N5 mutant.

Ultrastructure of Carboxysome from HCRM

A comparative study of the ultrastructure of carboxysomes in several HCRMs was carried out to help elucidate their proposed role in the CCM of cyanobacteria. Figure 3 shows a wild-type cell of *Synechococcus* PCC 7942 with the different stages of carboxysome development described above. Two HCRMs, M3 (Fig. 4, A and B) and EK6 (Fig. 4, C and D), showed a complete absence of mature carboxysomes and the exclusive presence of the carboxysome-resembling electron-clear inclusions (Table II). This suggests a correlation between the mature carboxysomes and the ability to grow at low CO_2 and supports our proposal that the electron-clear inclusions are an intermediate stage in the biogenesis of mature carboxysomes.

HCRM D4 exhibits mostly electron-clear inclusions but also shows carboxysomes with an internal electron-translucent area, ring-shaped structures, and typical carboxysomes (Fig. 4, E–G; Table II). Elongated bar-shaped carboxysomes were also observed occasionally (Table II). The low proportion of mature versus immature or atypical carboxysomes indicates a defect in the biogenesis of polyhedral bodies in this mutant.

The ultrastructure of the Km^r revertants EK20 and RK13, which are able to grow under low CO_2, was also studied. EK20 is a revertant of EK6 and RK13 is considered a revertant of D4 (Liemann-Hurwitz et al., 1991). We observed that both revertants possess normal-appearing carboxysomes (Fig. 5), correlating with their ability to grow under low CO_2.

HCRM N5 shows a noticeable increase in the number and the size of carboxysomes, with an appearance similar to that of typical polyhedral bodies of the wild type and, in

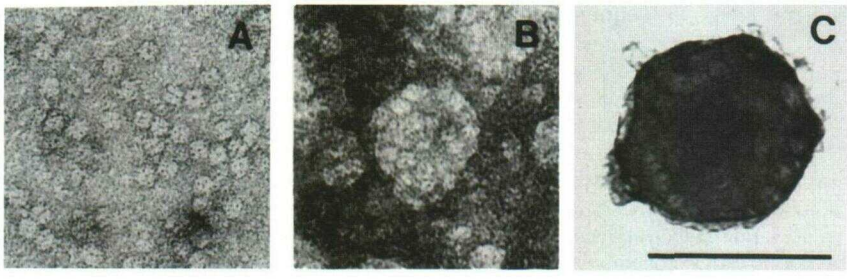

Figure 2. Transmission electron micrographs of negatively stained samples showing the assembly of Rubisco molecules. A, Free Rubisco molecules. B, Self assembly of Rubisco molecules. C, Carboxysome with internal Rubisco molecules. Bar = 100 nm.

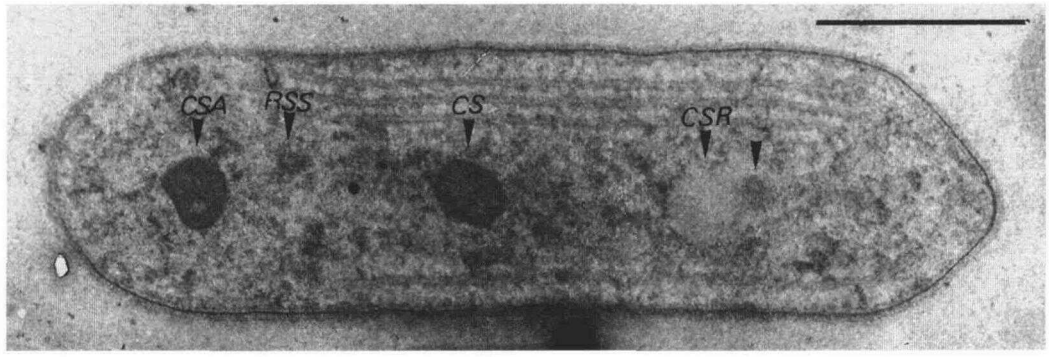

Figure 3. Transmission electron micrograph of a wild-type cell of *Synechococcus* PCC 7942. CS, Carboxysome; CSR, carboxysome-resembling electron-clear inclusion; CSA, carboxysome with internal electron-translucent area; RSS, ring-shaped structure. Bar = 500 nm. Cells were grown under high CO_2 and changed to low-CO_2 conditions 12 h before collection.

addition, a high frequency of elongated, variable-length carboxysomes, similar in width and electron density to normal carboxysomes (Fig. 4, H and I; Table II). This type of inclusion was also observed, but only rarely, in mutant D4 and revertants EK20 and EK13.

Throughout these ultrastructural studies, we noticed that many cells contained unusually dense granules of a more-or-less round shape. Cells with high, medium, and low numbers of granules appear simultaneously in the same sample. We speculated that their presence might be related to the time of adaptation to low-CO_2 conditions when we collected the cells. We have observed these granules in the wild type and in the four HCRMs studied, although with different frequency. The highest frequency of cells with high-medium numbers of granules correspond to mutants lacking mature carboxysomes, EK6 (92%) and M3 (75%), followed by D4 (63%) and by the wild type (40%). Only 23% of N5 cells show granules, and never in a high number. Cells with mature carboxysomes are usually free of these particles.

We analyzed the time course of the biochemical composition of cells during the first 24 h of adaptation to low CO_2. Figure 6 shows the cellular contents in total phycocyanins, Chl, and carbohydrates and the protein concentration of the carboxysomal extract of the wild-type cultures (low density of particles in the transmission electron micrographs) versus M3 and D4 cultures (high density of particles). The results do not show a substantial increase in phycobilisomes or glycogen in M3 or D4 in comparison with the wild type and throughout the adaptation period. For carboxysomal proteins, wild-type cells show an increase after 6 h, which corresponds with the induction of carboxysomes under low CO_2. By contrast, the mutants exhibit a transitory increase in carboxysomal proteins at 6 h followed by an immediate decrease to 0-time values. This time course can be interpreted as an unsuccessful attempt to build up new carboxysomes in response to low CO_2. Our data are consistent with the hypothesis that the granules have a protein composition and might be related to carboxysome biogenesis.

DISCUSSION

Carboxysome Maturation Stages

In this study structures related to the maturation of growing carboxysomes have been observed in wild-type cells. Figure 7 depicts these structures in order of their degree of maturity. The different-sized ring-shaped structures appear to be the earliest step in the assembly process (Figs. 1A and 7A). Next are the electron-clear carboxysomes (Figs. 1B and 7B), which lack a well-defined shell. The 12-nm diameter of the inner particles coincides with that of Rubisco molecules (Lanaras and Codd, 1981). Their orderly arrangement indicates that at this maturation stage Rubisco molecules have been assembled but that a carboxysome shell has not yet been laid out. The resemblance of these translucent carboxysomes to structures arising from Rubisco molecule self assembly (Fig. 2) and to negatively stained frozen hydrated carboxysomes (Holthuijzen et al., 1986), as well as scanning EM data (not shown), supports this interpretation. Carboxysomes with an electron-translucent area (Figs. 1C and 7C) suggest the assembly of the shell as the penultimate stage of carboxysome biogenesis.

These structures have also been observed in different HCRMs in which mature carboxysomes are missing (M3 and EK6) or scarce (D4). In these mutants the normal sequence of development is affected, hindering the final stages of development.

Price and Badger (1991) reported preliminary data on the biogenesis of carboxysomes in the filamentous cyanobac-

Figure 4. (On facing page). Transmission electron micrograph of HCRMs of *Synechococcus* PCC 7942. A and B, M3. C and D, EK6. E, F, and G, D4. H and I, N5. CS, Carboxysome; CSR, carboxysome-resembling electron-clear inclusion; CSA, carboxysome with internal electron-clear area; RSS, ring-shaped structure; BCS, bar-shaped carboxysome. Bar = 500 nm. Cells were grown under high CO_2 and changed to low-CO_2 conditions 12 h before collection.

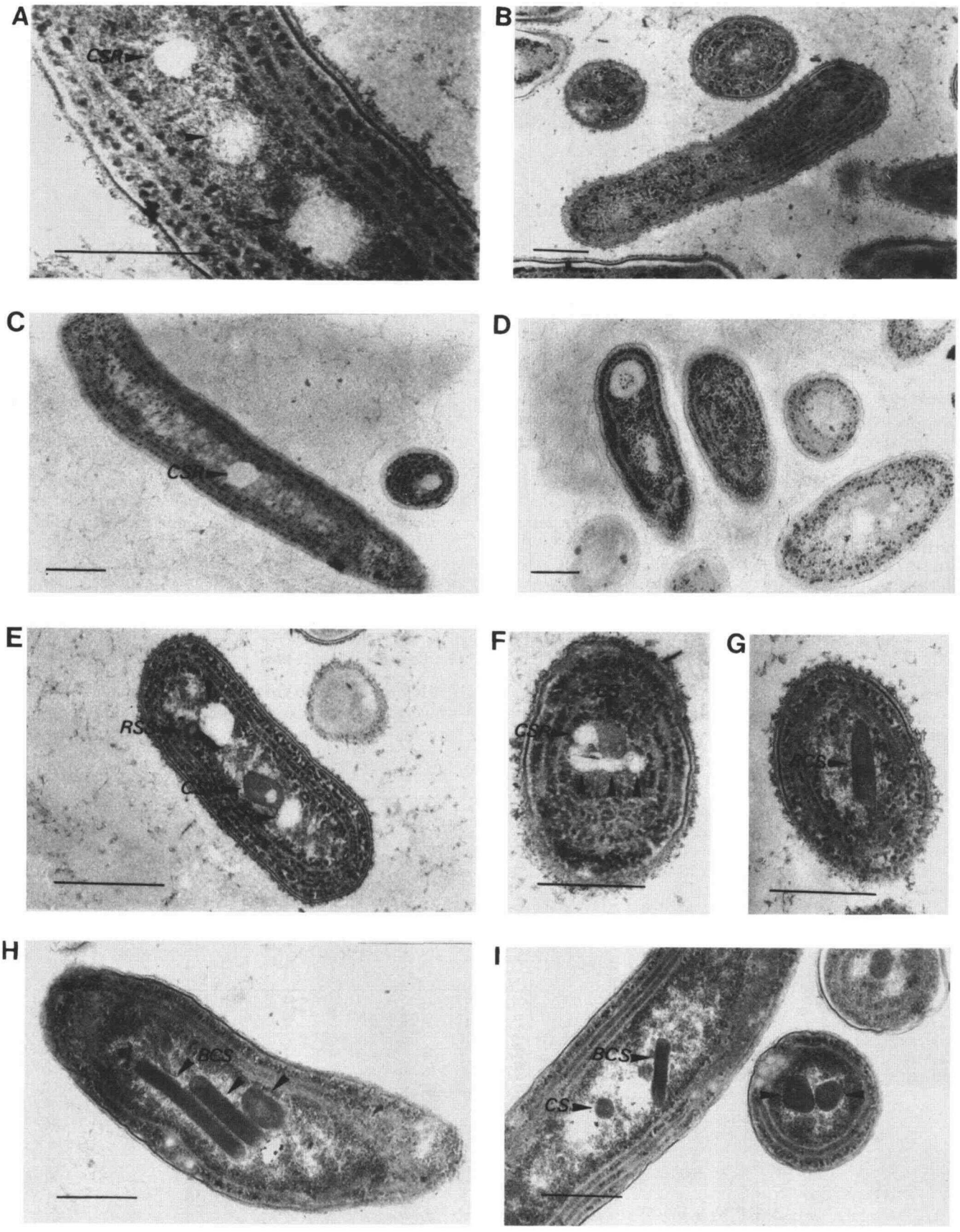

Figure 4. Legend appears on facing page.

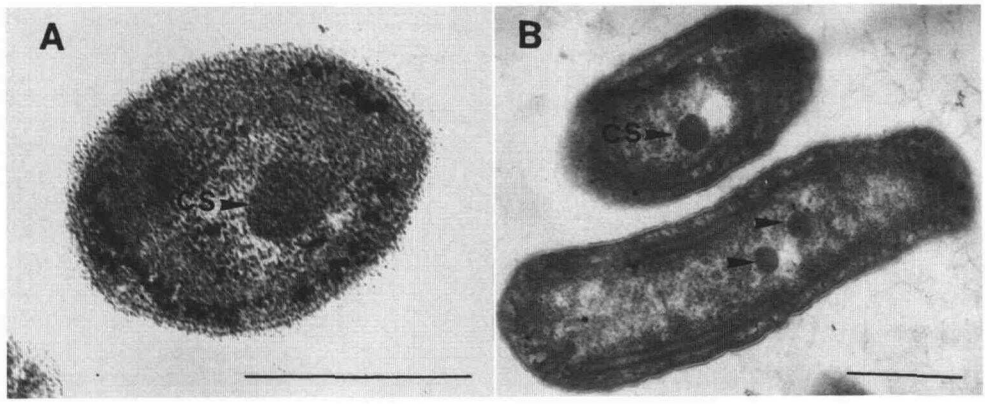

Figure 5. Transmission electron micrographs of revertants EK20 (A) and RK13 (B) of HCRMs EK6 and D4 of *Synechococcus* PCC 7942. CS, Carboxysome. Bar = 500 nm.

terium *Anabaena variabilis* M3. They observed small loose rings associated with mature carboxysomes and carboxysomes with a small translucent area, comparable to our stages A and C for *Synechococcus* PCC 7942. They proposed that the carboxysome shell is laid down first and that Rubisco would need to be inserted through this shell. Our observations include an intermediate stage (B), not reported in *Anabaena*, and suggest the alternative view that Rubisco (and perhaps other polypeptides) aggregates first and the shell is added as the last step. Price and Badger (1991) noted that the structures observed in *Anabaena* seemed to be absent in *Synechococcus*, suggesting either a different sequence of events in the latter or a more rapid progression to maturity due to their smaller cell size. Our observations of immature carboxysome stages in *Synechococcus* wild type can be ascribed to the fact that we examined the cells during the period of adaptation to low CO_2, when there is a significant increase in the number of carboxysomes (Turpin et at., 1984; McKay et al., 1993). It would be expected that immature stages appear during this period of active assembly of new carboxysomes. We have also observed carboxysomes with an electron-translucent area (type C) in *Anabaena* cells grown under severe limitation of C_i induced by Na^+ deficiency (E. Fernández-Valiente, personal communication), in *Synechococcus* (Friedberg et al., 1989; Kaplan, 1990), and in *Synechocystis* (Ogawa et al., 1994), although such structures had not been pointed out by the various authors cited.

Carboxysomes of HCRMs

Mutants unable to grow at low concentrations of C_i are a powerful tool that can be used to elucidate the physiological and molecular basis of the operation of the CCM.

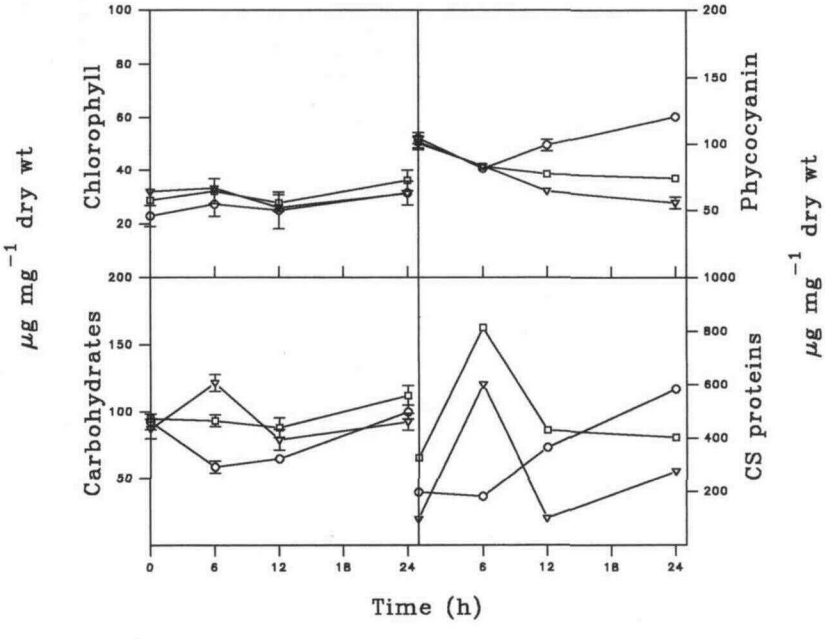

Figure 6. Time course of the cellular concentration on Chl, phycocyanin, carbohydrate, and carboxysomal proteins in *Synechococcus* PCC 7942 wild type (○), HCRM M3 (▽), and HCRM D4 (□) upon transfer from high- (0 time) to low-CO_2 conditions.

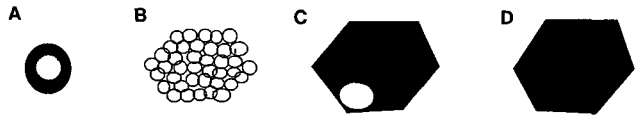

Figure 7. Model depicting the different stages of carboxysome formation found in *Synechococcus* PCC 7942 and micrographed in Figure 1, arranged according to their proposed maturation degree.

Several mutants in which the requirement for high CO_2 for growth coincides with anomalous carboxysomes have been described. A mutant of *Synechococcus* PCC 7942 P/N (Price and Badger, 1991) lacks carboxysomes, whereas O221 (Friedberg et al., 1989) and N1 (Marco et al., 1994) show diffuse or aberrant carboxysomes. The genomic lesions map within three of the ORFs identified upstream of the region of the *rbcLS* operon, namely *ccmM*, *ccmN*, and *ccmO*. Thus, this gene cluster seems to be involved in the structure/assembly of carboxysomes. Indeed, *ccmO* has significant sequence similarity with the gene encoding the major carboxysome shell peptide in the chemolithotrophic bacteria *Thiobacillus neapolitanus*, which was recently identified by English et al. (1994).

Our findings point to other ORFs of the *rbcLS* region not directly clustered with *ccmM*, *ccmN*, *ccmO* as also participating, directly or indirectly, in the correct assembly of these inclusions. M3 is an HCRM obtained by insertion of a Km^r cartridge at the *Eco*RI site 7.5 kb upstream of *rbcLS* (Schwarz et al., 1992b). The ORF78 and 68 identified within the two strands of this DNA fragment do not show any significant homology to any known gene. The lack of mature carboxysomes in M3 is evidence in favor of the role of carboxysomes as the site of CO_2 elevation, since this mutant exhibits a very low apparent photosynthetic affinity for external C_i in spite of being able to accumulate C_i in the cytoplasm.

The genetic lesion of EK6 is completely different from that of M3. It consists of an 84-bp insertion near the 3′ end of *rbcS*, leading to a 17-kD small subunit of Rubisco instead of the 14-kD normal subunit (Liemann-Hurwitz et al., 1991). The altered structure of the enzyme results in an apparent photosynthetic affinity for C_i 50-fold lower than that in the wild type. However, the requirement for high CO_2 for the growth of this mutant does not seem to be related to a failure of the carboxylating activity of the enzyme itself, which was similar to that of wild type in crude extract measurements (Lieman-Hurwitz et al., 1991). Our ultrastructural study has revealed that this mutant, similar to M3, lacks carboxysomes and shows immature electron-translucent inclusions. In *T. neapolitanus*, Holthuijzen et al. (1986) concluded that Rubisco small subunit is involved in the assembly of the carboxysome shell peptides. On the other hand, the substitution of the *Synechococcus* original Rubisco gene by that of the photosynthetic bacterium *Rhodospirillum rubrum*, which lacks both the small subunit and carboxysomes, led to an HCRM without carboxysomes (Pierce et al., 1989). Therefore, there is an obvious correlation between the EK6 genetic lesion and its inability to build up mature carboxysomes, whether or not the catalytic activity of the enzyme is modified. EK20, a revertant of EK6 that retains the Km^r insert but is able to grow at low CO_2 (Liemann-Hurwitz et al., 1991), does possess mature carboxysomes.

Mutant D4 provides an example of how the alteration of an apparently unrelated gene, of an enzyme in the purine biosynthesis pathway, can affect carboxysomes. The ORF involved is located immediately downstream of *rbcLS* (Liemann-Hurwitz et al., 1991) and shows significant homology with bacterial *purK* (Schwarz et al., 1992a), a subunit of phosphoribosyl aminoamidazole carboxylase that is required for the operation of the enzyme only under low-CO_2 conditions. Neither the capacity to accumulate C_i nor the apparent photosynthetic affinity for external C_i are seriously affected in this mutant (Schwarz et al., 1992a). We have observed that most of its carboxysomes are immature electron-translucent ones, but that it also exhibits carboxysomes with an electron-translucent area and the typical polyhedral bodies. The preponderance of the immature forms means that development of carboxysomes is slowed down in D4, which explains its HCRM phenotype. An alternative explanation is the predicted decrease in cellular purine levels under low CO_2 (Schwarz et al., 1992a). We cannot provide any evidence to link the failure in purine biosynthesis with that of carboxysome assembly.

RK13, which can be considered a revertant of D4 (Liemann-Hurwitz et al., 1991), grows under low CO_2 and exhibits typical carboxysomes. This case, similar to that described above for EK6/EK20, proves that the restoration of the ability to grow under low CO_2 is accompanied by a renewed ability to assemble carboxysomes. This implies that carboxysomes are essential for the operation of the CCM and that genetic lesions affecting their maturity lead to the HCRM phenotype.

The mutation of N5 is located in *ndhB*, which encodes subunit II of NADH dehydrogenase, and causes a failure in the energization of C_i transport. Accordingly, these cells are unable to accumulate C_i and to survive under low-CO_2 conditions (Marco et al., 1993). Our finding of a markedly increased number of fully developed carboxysomes in this mutant, most of them of enlarged size, indicates that the failure in one of the first steps of the CCM—concentrating C_i internally—leads to an enlarged response in a subsequent step: increasing the number and size of the sites of CO_2 elevation, the carboxysomes. Such increased synthesis of carboxysome precursors might result in their assembly into the bar-shaped carboxysomes frequently found in this mutant. Bar-shaped carboxysomes have been reported in HCRM type I and PVU (Price and Badger, 1991) and E1 (Friedberg et al., 1989) and have been interpreted as aberrant bodies resulting from the alteration of *ccmL*. However, this type of carboxysome coexists with typical carboxysomes in the same cell and have also been found in wild-type *Synechococcus* under conditions of predictable severe stress for C_i, such as stationary-phase old cultures (Gantt and Conti, 1969) and cultures bubbled with 30 μL of CO_2 in air at pH 9.5 (McKay et al., 1993). Thus, we propose that bar-shaped carboxysomes might be, rather than the result of a genomic lesion, the consequence of increased or un-

balanced synthesis of carboxysome precursors favoring an unbalanced assembly pathway resulting in these giant bodies. Ultrastructural data on other HCRM mutants impaired in C_i transport, such as those of *Synechocystis* (Ogawa, 1992) and *Synechococcus* (Yu et al., 1994), could be very useful in further studies of carboxysome assembly and verification of the model proposed herein.

ACKNOWLEDGMENTS

The authors wish to thank Prof. A. Kaplan for providing the mutants, E. Fernández-Valiente for helpful discussions, J. Wierzchos for electron back-scattered scanning EM technique, and J.R. Benemann for critical review of the manuscript.

Received November 16, 1994; accepted December 13, 1994.

LITERATURE CITED

Badger MR (1980) Kinetic properties of ribulose 1,5-bisphosphate carboxylase/oxygenase from *Anabaena variabilis*. Arch Biochem Biophys **201:** 247–254

Badger MR, Price GD (1992) The CO_2 concentrating mechanism in cyanobacteria and microalgae. Physiol Plant **84:** 606–615

Blumwald E, Tel-Or E (1982) Osmoregulation and cell composition in salt adaptation of *Nostoc muscorum*. Arch Microbiol **132:** 169–172

Bradford MM (1976) A rapid and sensitive method for the quantitation of microgram quantities of protein utilizing the principle of protein-dye binding. Anal Biochem **72:** 248–254

Dubois M, Gilles RA, Hamilton JK, Rubers PA, Smith F (1956) Colorimetric method for determination of sugar and related substances. Anal Chem **28:** 350–356

English RS, Lorbach SC, Qin X, Shively JM (1994) Isolation and characterization of a carboxysome shell gene from *Thiobacillus neapolitanus*. Mol Microbiol **12:** 647–654

Friedberg D, Kaplan A, Ariel R, Kessel M, Seijffors J (1989) The 5′-flanking region of the gene encoding the large subunit of ribulose-1,5-bisphosphate carboxylase/oxygenase is crucial for growth of the cyanobacterium *Synechococcus* sp. strain PCC 7942 at the level of CO_2 in air. J Bacteriol **171:** 6069–6076

Fukuzawa H, Suzuki E, Komukai Y, Miyachi S (1992) A gene homologous to chloroplast carbonic anhydrase (*icfA*) is essential to photosynthetic carbon dioxide fixation by *Synechococcus* PCC 7942. Proc Natl Acad Sci USA **89:** 4437–4441

Gantt E, Conti SF (1969) Ultrastructure of blue-green algae. J Bacteriol **97:** 1486–1493

Holthuijzen YA, Van Breemen JFL, Gijs Kuenen J, Konings WN (1986) Protein composition of the carboxysomes of *Thiobacillus neapolitanus*. Arch Microbiol **144:** 398–404

Kaplan A (1990) Analysis of high-CO_2-requiring mutants indicates a central role for the 5′-flanking region of *rbc* and for the carboxysomes in cyanobacterial photosynthesis. Can J Bot **68:** 1303–1310

Kaplan A, Schwarz R, Lieman-Hurwitz J, Ronen-Tarazi M, Reinhold L (1994) Physiological and molecular studies on the response of cyanobacteria to changes in the ambient inorganic carbon concentration. *In* DA Bryant, ed, The Molecular Biology of Cyanobacteria. Kluwer Academic Publishers, Dordrecht, The Netherlands, pp 469–485

Lanaras T, Codd GA (1981) Ribulose-1,5-bisphosphate carboxylase and polyhedral bodies of *Chlorogloeopsis fritschii*. Planta **153:** 279–285

Lieman-Hurwitz J, Schwarz R, Martínez F, Maor Z, Reinhold L, Kaplan A (1991) Molecular analysis of high CO_2 requiring mutants: involvement of genes in the region of *rbc*, including *rbcS*, in the ability of cyanobacteria to grow under low CO_2. Can J Bot **69:** 945–950

Marco E, Martínez I, Ronen-Tarazi M, Orús MI, Kaplan A (1994) Inactivation of *ccmO* in *Synechococcus* sp. strain PCC 7942 results in a mutant requiring high levels of CO_2. Appl Environ Microbiol **60:** 1018–1020

Marco E, Ohad N, Schwarz R, Lieman-Hurwitz J, Gabay C, Kaplan A (1993) High CO_2 concentration alleviates the block in photosynthetic electron transport in an *ndhB*-inactivated mutant of *Synechococcus* sp. PCC 7942. Plant Physiol **101:** 1047–1053

Marker AFM (1972) The use of acetone and methanol in the estimation of chlorophyll in the presence of phaeophytin. Freshwater Biol **2:** 361–385

McKay RML, Gibbs SP, Espie GS (1993) Effect of dissolved inorganic carbon on the expression of carboxysomes, localization of Rubisco and the mode of inorganic carbon transport in cells of the cyanobacterium *Synechococcus* UTEX 625. Arch Microbiol **159:** 21–29

Ogawa T (1992) NAD(P)H dehydrogenase: a component of PS-I cyclic electron flow driving inorganic transport in cyanobacteria. *In* N Murata, ed, Research in Photosynthesis, Vol III. Kluwer Academic Publishers, Dordrecht, The Netherlands, pp 763–770

Ogawa T, Marco E, Orús MI (1994) A gene (*ccmA*) required for carboxysome formation in the cyanobacterium *Synechocystis* sp. strain PCC6803. J Bacteriol **176:** 2374–2378

Orús MI, Marco E (1993) Trichlorfon-induced inhibition of nitrate and ammonium uptake in cyanobacteria. J Exp Bot **44:** 501–508

Pierce J, Carlson TJ, Williams JGK (1989) A cyanobacterial mutant requiring the expression of ribulose bisphosphate carboxylase from a photosynthetic anaerobe. Proc Natl Acad Sci USA **86:** 5753–5757

Price GD, Badger MR (1991) Evidence for the role of carboxysomes in the cyanobacterial CO_2-concentrating mechanism. Can J Bot **69:** 963–973

Price GD, Coleman JR, Badger MR (1992) Association of carbonic anhydrase with carboxysomes isolated from the cyanobacterium *Synechococcus* PCC 7942. Plant Physiol **100:** 784–793

Reinhold L, Kosloff R, Kaplan A (1991) A model for inorganic carbon fluxes and photosynthesis in cyanobacterial carboxysomes. Can J Bot **69:** 984–988

Reinhold L, Zviman M, Kaplan A (1989) A quantitative model for inorganic carbon fluxes and photosynthesis in cyanobacteria. Plant Physiol Biochem **27:** 945–954

Rippka R (1988) Isolation and purification of cyanobacteria. Methods Enzymol **167:** 3–27

Schwarz R, Lieman-Hurwitz J, Hassidim M, Kaplan A (1992a) Phenotypic complementation of high CO_2-requiring mutants of the cyanobacterium *Synechococcus* sp. strain PCC 7942 by inosine 5′-monophosphate. Plant Physiol **100:** 1987–1993

Schwarz R, Lieman-Hurwitz J, Marco E, Ronen-Tarazi M, Ohad N, Hassidim M, Gabay C, Reinhold L, Kaplan A (1992b) The CO_2-concentrating mechanism of cyanobacteria: elucidation with the aid of high-CO_2-requiring mutants. *In* N Murata, ed, Research in Photosynthesis, Vol III. Kluwer Academic Publishers, Dordrecht, The Netherlands, pp 437–440

Turpin DH, Miller AG, Canvin DT (1984) Carboxysome content of *Synechococcus leopliensis* (Cyanophyta) in response to inorganic carbon. J Phycol **20:** 249–253

Yu JW, Price GD, Badger MR (1994) A mutant isolated from the cyanobacterium *Synechococcus* PCC 7942 is unable to adapt to low inorganic carbon conditions. Plant Physiol **104:** 605–611

Yu JW, Price GD, Song L, Badger MR (1992) Isolation of a putative carboxysomal carbonic anhydrase gene from the cyanobacterium *Synechococcus* PCC 7942. Plant Physiol **100:** 794–800